

Band alignment of Al_2O_3 with (-201) $\beta\text{-Ga}_2\text{O}_3$

Patrick H. Carey IV^a, F. Ren^a, David C. Hays^b, B.P. Gila^b, S.J. Pearton^{b,*}, Soohwan Jang^c, Akito Kuramata^{d,e}

^a Department of Chemical Engineering, University of Florida, Gainesville, FL 32611, USA

^b Department of Materials Science and Engineering, University of Florida, Gainesville, FL 32611, USA

^c Department of Chemical Engineering, Dankook University, Yongin 16890, South Korea

^d Tamura Corporation, Sayama, Saitama 350-1328, Japan

^e Novel Crystal Technology, Inc., Sayama, Saitama 350-1328, Japan

ARTICLE INFO

Article history:

Received 10 April 2017

Received in revised form

3 May 2017

Accepted 5 May 2017

Available online 6 May 2017

ABSTRACT

X-Ray Photoelectron Spectroscopy was used to determine the valence band offset at $\text{Al}_2\text{O}_3/\beta\text{-Ga}_2\text{O}_3$ heterointerfaces. The Al_2O_3 was deposited either by Atomic Layer Deposition (ALD) or rf magnetron sputtering and the synthesis method was found to have a very significant effect on the resulting band alignment. The bandgaps of the materials were determined by Reflection Electron Energy Loss Spectroscopy as 4.6 eV for Ga_2O_3 and 6.9eV for Al_2O_3 deposited by either method. The valence band offset was determined to be $0.07\text{eV} \pm 0.20\text{ eV}$ (straddling gap, type I alignment) for ALD Al_2O_3 on Ga_2O_3 and $-0.86 \pm 0.25\text{ eV}$ (staggered gap, type II alignment) for sputtered Al_2O_3 . This led to conduction band offsets of $2.23 \pm 0.60\text{ eV}$ for ALD Al_2O_3 and $3.16 \pm 0.80\text{ eV}$ for sputtered Al_2O_3 , respectively. The choice of deposition method for the dielectric alters the type of band alignment for the $\text{Al}_2\text{O}_3/\text{Ga}_2\text{O}_3$ system from type I alignment to type II. Since the main difference is expected to be the disorder at the dielectric/ Ga_2O_3 interface, this shows how synthesis method can affect the resulting band alignment.

© 2017 Elsevier Ltd. All rights reserved.

1. Introduction

The β -polymorph of Ga_2O_3 is attracting interest for high power switching electronics, solar-blind UV photodetectors and sensors. Ga_2O_3 is commercially available in large diameter, bulk single-crystal form and impressive demonstrations of high quality epi grown by Hydride Vapor Phase Epitaxy (HVPE) and Metal Organic Chemical Vapor Deposition (MOCVD) have been reported [1–13]. The large bandgap of Ga_2O_3 means that it has a theoretical breakdown field of $\sim 8\text{ MV cm}^{-1}$, which is higher than either GaN or SiC [4,8]. This leads to high theoretical power electronics figures-of-merit [4,6,8–11,14]. Different types of Ga_2O_3 -based power rectifiers and transistors have been reported [4,6–17]. Both metal-semiconductor field effect transistors (MESFETs) and metal-oxide–semiconductor field effect transistors (MOSFETs) have been reported for Ga_2O_3 [7,8,11,12,15–17]. It is desirable to have metal-oxide-semiconductor (MOS) gates on transistors for improved thermal stability, threshold voltage control and lower interface

state density than with metal gates [4,6,11,18–20]. The gate dielectrics employed to date [21–26] have typically been either Atomic Layer Deposited (ALD) or Pulsed Laser Deposited (PLD) Al_2O_3 or HfO_2 , [8,11,12,22–24] along with Plasma Enhanced Chemical Vapor Deposited SiO_2 [4,6,21,25].

Since a gate dielectric must act as a barrier to both electrons and holes and because band discontinuities can form a barrier for carrier transport across the interface, the knowledge of heterointerface band alignment is essential for predicting the transport properties of the interface, or the electrostatic potential in a heterojunction device. Materials with a high dielectric constant (high-K) are desirable for Ga_2O_3 MOSFETs, since the higher capacitance can reduce the effect of interface traps, and therefore reduce the device operating voltage [4,6,21–24]. However, many of the high-K dielectrics available are often synthesized in polycrystalline form, which is undesirable due to impurity diffusion through grain boundaries and there are fewer choices with sufficiently high bandgap to get the desired $>1\text{ eV}$ conduction and valence band offsets [4,11,12]. Kamimura et al. [22] measured a band gap of $6.8 \pm 0.2\text{ eV}$ for ALD Al_2O_3 and the conduction and valence band offsets at the interface were estimated to be $1.5 \pm 0.2\text{ eV}$ and $0.7 \pm 0.2\text{ eV}$, respectively. Hung et al. used capacitance-voltage

* Corresponding author.

E-mail address: spear@mse.ufl.edu (S.J. Pearton).

profiling on ALD $\text{Al}_2\text{O}_3/\beta\text{-Ga}_2\text{O}_3$ interfaces and found a conduction band offset of 1.7 eV. Hattori et al. [24] measured conduction and valence band offsets of 1.9 and 0.5 eV, respectively for high quality epitaxial films of $\gamma\text{-Al}_2\text{O}_3$ deposited by PLD on single-crystal Ga_2O_3 . Thus there is a difference of 0.4–0.6 eV in the reported conduction band offsets for Al_2O_3 on Ga_2O_3 for well-controlled dielectric deposition methods. In a similar vein for other dielectrics on Ga_2O_3 , Konishi et al. [21] obtained a conduction band offset of 3.1 ± 0.2 eV and a corresponding valence band offset of 1.0 ± 0.2 eV for the $\text{SiO}_2/\text{Ga}_2\text{O}_3$ interface where the dielectric deposition was by PECVD. Jia et al. [25] got a much smaller valence band offset (0.43 eV) measured with X-Ray Photoelectron Spectroscopy (XPS) for SiO_2 deposited by ALD on single crystal $\beta\text{-Ga}_2\text{O}_3$, with a corresponding larger conduction band offset of 3.63 eV. Wheeler et al. [26] measured the band alignment between ALD ZrO_2 or HfO_2 and $\beta\text{-Ga}_2\text{O}_3$ and both dielectrics resulted in a type II, staggered gap alignment with a conduction band offset of 1.2 and 1.3 eV for ZrO_2 and HfO_2 films, respectively.

There is typically variability reported in the literature for both valence and conduction band offsets for dielectrics on electronic oxides or semiconductors [26–28]. Some of the causes include metal contamination, interface disorder, dielectric composition, carbon/hydrogen contamination, annealing, stress/strain and surface termination [27,28]. The presence of these effects can result in differences in the bandgap of the dielectric and this affects the conduction band offset since the valence band offset is directly measured. However, the latter can also be affected by most of these same issues [29]. A comparison of ALD deposited dielectrics with sputtered films allows us to identify mechanisms that can lead to differences in band alignment.

In this paper, we report on the determination of the band alignment in the $\text{Al}_2\text{O}_3/\text{Ga}_2\text{O}_3$ heterostructure, in which the Al_2O_3 was deposited by either ALD or sputtering. We employ X-Ray Photoelectron Spectroscopy (XPS) to determine the valence band offsets and by measuring the respective bandgaps of the Al_2O_3 (6.9 eV) and Ga_2O_3 (4.6 eV), we were also able to determine the conduction band offset in $\text{Al}_2\text{O}_3/\text{Ga}_2\text{O}_3$ heterostructures and show that the dielectric deposition method has a very large effect on the band alignment.

2. Experimental

The bulk β -phase Ga_2O_3 single crystals with (-201) surface orientation (Tamura Corporation, Japan) were grown by the edge-defined film-fed growth method. Hall effect measurements showed the sample was unintentionally n-type with an electron concentration of $\sim 3 \times 10^{17} \text{ cm}^{-3}$. The samples were cleaned using UV/ozone exposure and solvent rinses prior to insertion into the RF magnetron sputtering or ALD systems used for Al_2O_3 deposition. The sputtering was carried out at room temperature using a 3-in. diameter target of pure Al. The RF power was 350 W and the working pressure was 5 mTorr in a 3% O_2/Ar ambient. The ALD layers were deposited at 200 °C in a Cambridge Nano Fiji 200 using a trimethylaluminum source and a remote inductively coupled plasma (ICP) at 300 W to generate atomic oxygen. Plasma mode ALD helps lower contaminants in the film and reduces the nucleation delay while minimizing ion induced damage by utilizing a remote source. Both thick (200 nm) and thin (1.5 nm) layers of the Al_2O_3 were deposited by both methods to allow measurement of both bandgaps and core levels on the $\beta\text{-Ga}_2\text{O}_3$ [30–32].

To obtain the valence band offsets, XPS survey scans were performed to determine the chemical state of the Al_2O_3 and Ga_2O_3 and identify peaks for high resolution analysis [30,31]. A Physical Electronics PHI 5100 XPS with an aluminum x-ray source (energy 1486.6 eV) with source power 300 W was used, with an analysis

area of $2 \text{ mm} \times 0.8 \text{ mm}$, a take-off angle of 50° and an acceptance angle of $\pm 7^\circ$. The electron pass energy was 23.5 eV for the high resolution scans and 187.5 eV for the survey scans. The samples were exposed to ambient when transferred to the XPS system and thus the surface will have carbon resulting from this exposure. Greczynski and Hultman [33] have recently shown that using this carbon as a binding energy reference, which is the commonly used approach, can actually be subject to significant error.

Charge compensation was performed using an electron flood gun. The charge compensation flood gun is often not sufficient at eliminating all surface charge, and additional corrections must be performed. Using the known position of the adventitious carbon (C-C) line in the C 1s spectra at 284.8 eV, charge correction was performed. During the measurements, all the samples and electron analyzers were electrically grounded so they were performed providing a common reference Fermi level. Differential charging is a serious concern for photoemission dielectric/semiconductor band offset measurements [32,33]. While the use of an electron flood gun does not guarantee that differential charging is not present and in some cases could make the problem worse, our experience with oxides on conducting substrates has been that the differential charging is minimized with the use of an electron gun. Calibrations with and without the gun and verified that was the case. This procedure has been described in detail previously [28,29]. However, as discussed earlier, the use of referencing against the C 1s peak is not always a reliable approach [33].

Reflection electron energy loss spectroscopy (REELS) was employed to measure the bandgaps of the Al_2O_3 and Ga_2O_3 . REELS is a surface sensitive technique capable of analyzing electronic and optical properties of ultrathin gate oxide materials because the low-energy-loss region reflects the valence and conduction band structures [32]. REELS spectra were obtained using a 1 kV electron beam and the hemispherical electron analyzer.

3. Results and discussion

Fig. 1 shows the stacked XPS survey scans of thick (200 nm) sputtered and ALD deposited Al_2O_3 , 1.5 nm ALD or sputtered Al_2O_3 on Ga_2O_3 and finally, the bulk Ga_2O_3 crystals. The spectra are free from metal contaminants and consistent with past published XPS data on these materials [25,26,34]. In particular, we looked

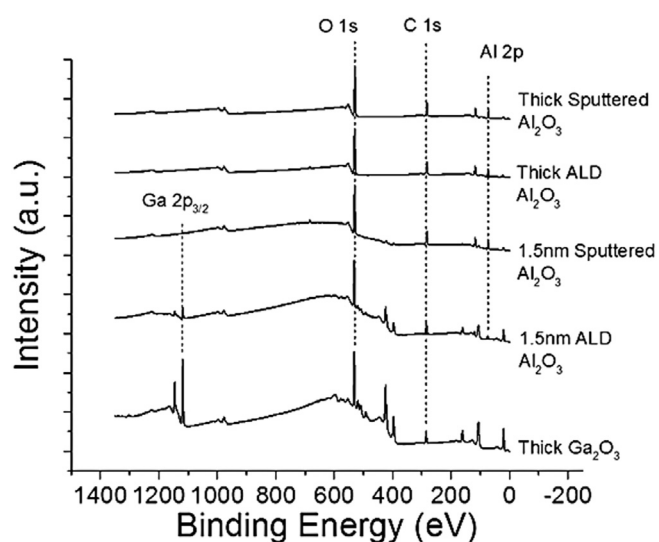


Fig. 1. XPS survey scans of thick sputtered or ALD Al_2O_3 , 1.5 nm sputtered or ALD Al_2O_3 on Ga_2O_3 and Ga_2O_3 bulk sample.

carefully for the presence of metallic contaminants in the sputtered films whose oxides might lower the overall bandgap of the Al_2O_3 and thus affect the band alignment. However these were not detected to the sensitivity level of XPS. There is the presence of adventitious carbon from the atmospheric exposure of the samples during transfer between the various deposition tools and the XPS system.

The valence band maximum (VBM) was determined by linearly fitting the leading edge of the valence band and the flat energy distribution from the XPS measurements, and finding the intersection of these two lines [30], as shown in Fig. 2 for the bulk Ga_2O_3 (top) and thick Al_2O_3 (bottom). The VBM was measured to be 3.2 ± 0.2 eV for Ga_2O_3 , which is consistent with previous reports [21–23,30] and 3.25 ± 0.3 eV for the ALD Al_2O_3 or 2.58 ± 0.3 eV for the sputtered Al_2O_3 . The shift in these levels for the different synthesis techniques indicates the likely presence of interfacial disorder caused by the sputtering [35–41].

The bandgap of the Ga_2O_3 was determined to be 4.6 ± 0.3 eV, as shown in the REELS spectra in Fig. 3 (top). The band gap was determined from the onset of the energy loss spectrum [32]. The

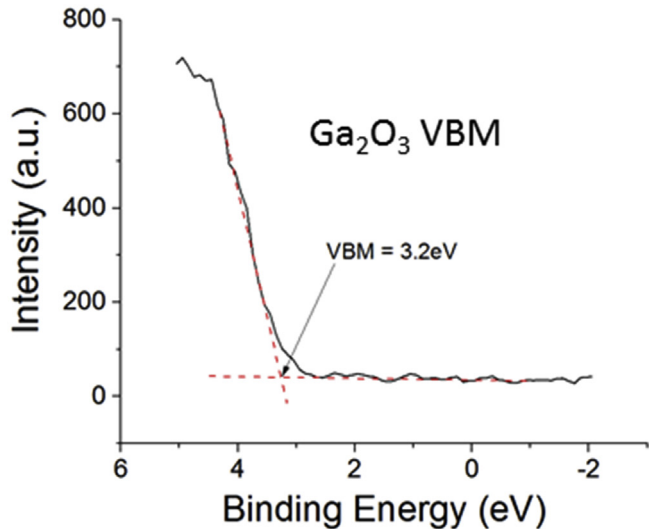


Fig. 2. XPS spectra of core levels to valence band maximum (VBM) for bulk Ga_2O_3 (top) and thick film Al_2O_3 deposited by either sputtering or ALD (bottom).

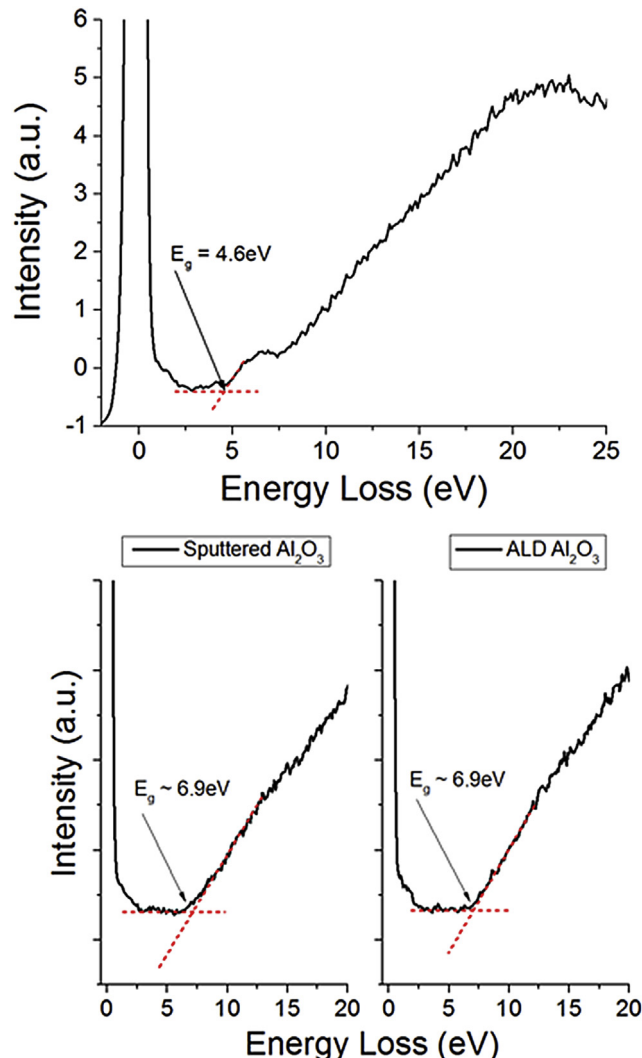


Fig. 3. (top) Reflection electron energy loss spectra to determine the bandgap of bulk Ga_2O_3 (top) and for thick ALD or sputtered Al_2O_3 (bottom).

measured band gap for both the sputtered and ALD Al_2O_3 was 6.9 ± 0.6 eV from the REELS data of Fig. 3 (bottom), which is consistent with literature values. The difference in bandgaps between Al_2O_3 and Ga_2O_3 is therefore 2.3 eV. To determine the actual band alignment and the respective valence and conduction band offsets, we examined the core level spectra for the samples.

High resolution XPS spectra of the VBM-core delta region are shown in Fig. 4 for the Ga_2O_3 (top) and thick sputtered and ALD Al_2O_3 (bottom) samples. Once again, there was a difference for the two types of Al_2O_3 films. Fig. 5 shows the XPS spectra for the Ga_2O_3 to Al_2O_3 -core delta regions of the two types of heterostructure samples. These values are summarized in Table 1 for the three samples examined and these were then inserted into the following equation to calculate ΔE_V [42–46]:

$$\Delta E_V = (E_{\text{Core}} - E_{\text{VBM}})_{\text{Ref. } \text{Ga}_2\text{O}_3} - (E_{\text{Core}} - E_{\text{VBM}})_{\text{Ref. } \text{Al}_2\text{O}_3} - (E_{\text{Core}}^{\text{Ga}_2\text{O}_3} - E_{\text{Core}}^{\text{Al}_2\text{O}_3})_{\text{Ga}_2\text{O}_3}^{\text{Al}_2\text{O}_3}$$

In this equation, the reference Ga_2O_3 and Al_2O_3 subscripts refer to the core and valence band maxima in the "thick" samples of each, whereas the last term refers to the core energy levels measured in

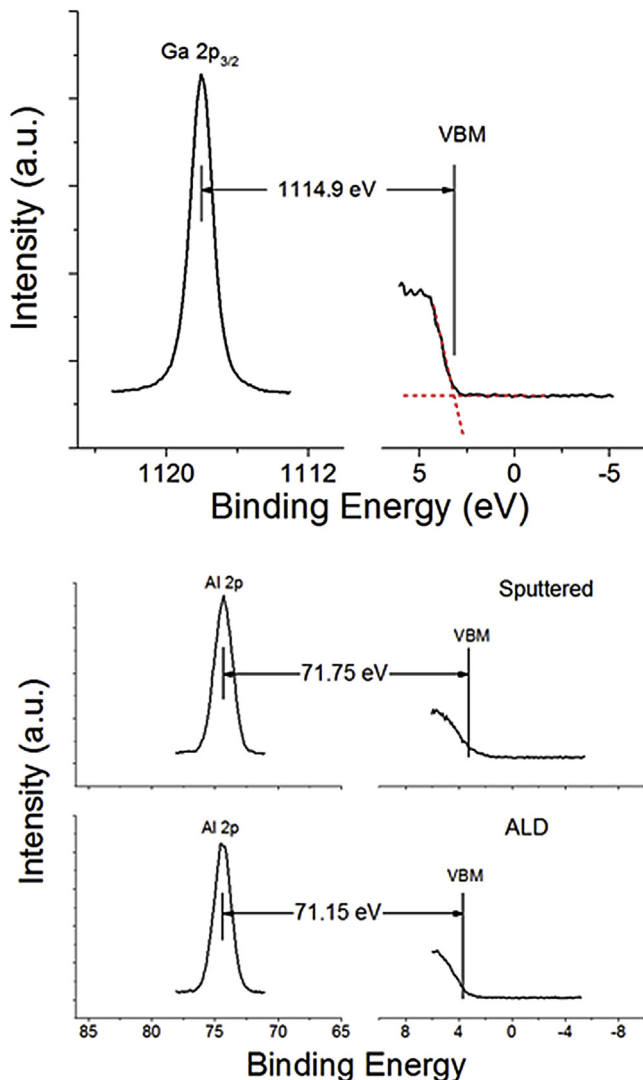


Fig. 4. High resolution XPS spectra for the vacuum-core delta regions of (top) the bulk Ga_2O_3 (top) and sputtered or ALD Al_2O_3 (bottom).

the composite sample with thin Al_2O_3 on bulk Ga_2O_3 .

Fig. 6 shows the band diagrams of the $\text{Al}_2\text{O}_3/\text{Ga}_2\text{O}_3$ heterostructure for both types of Al_2O_3 . Our data shows the alignment is a nested, type I alignment for the ALD Al_2O_3 , with a valence band offset of 0.07 ± 0.20 eV and the conduction band offset is then 2.23 ± 0.6 eV using the following equation: $\Delta E_C = E_g^{\text{Al}_2\text{O}_3} - E_g^{\text{Ga}_2\text{O}_3} - \Delta E_V$, i.e. $\Delta E_C = 6.9\text{eV} - 4.6\text{eV} - 0.07\text{eV} = 2.23\text{eV}$. Note that the error bar in the valence band offset means it could still be a staggered type II interface, but the main point is that the magnitude of the valence band offset is very small.

By sharp contrast, the sputtered film has a staggered, type II alignment with Ga_2O_3 , with a valence band offset of -0.86 eV and a conduction band offset of 3.16 eV. It is known that sputtered films containing metallic contaminants and interfacial disorder due to the sputter-induced damage [36–42], suffer from Fermi level pinning effects and are less likely to be accurate than a more controlled process such as ALD with a more abrupt interface and far fewer expected defects. In our case, we know that contamination is not a significant problem and thus the main contributor is surface-induced disorder. A number of papers have reported on the presence of interfacial defects, such as oxygen or metal atom vacancies, and the effect that they can have on the band offsets of

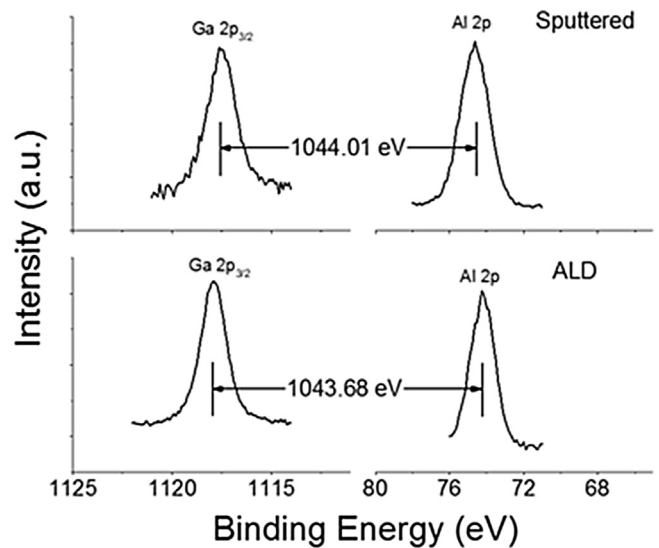


Fig. 5. High resolution XPS spectra for the Ga_2O_3 to Al_2O_3 -core delta regions for both types of Al_2O_3 .

materials [35–43]. The literature shows that energy band alignment variations of sometimes more than 1 eV depending on interface preparation can be obtained [35–39,45,46], due to the presence of high defect concentrations in the materials and on a cation effect that will increase the VBM of that material. Modeling has shown that the defect density has to be at least $10^{12} \text{ e}^-/\text{cm}^2$ to produce significant shifts [36]. Defect densities of this magnitude will produce a shift up or down, depending on the sign of the charge, of ~ 0.3 eV. We see a substantial shift of the VBM for the sputtered material to higher energies by 0.60 eV.

These band alignments differences for the same heterostructure are a strong function of the deposition methods, where, for example, sputtering may create more interfacial disorder and have metallic contamination that alters the bandgap of the dielectric. The literature on band alignments on β - Ga_2O_3 is not yet extensive enough to draw those conclusions for this material, but already variations have been reported for nominally similar dielectrics. Kamimura et al. [22] reported a valence band offset of 0.7 ± 0.2 eV for ALD Al_2O_3 on Ga_2O_3 using similar deposition conductions to those used in our work. They showed the presence of a significant density of border traps in their Al_2O_3 from capacitance-voltage data, but the differences with our results show that even nominally similar dielectric deposition conditions can still lead to variations in reported band alignments. Similarly, Hattori et al. obtained a valence band offset of 0.5 eV for this interface when using PLD Al_2O_3 . Their electrical measurements found a high interface trap density at the interface, which was also the case in ALD $\text{Al}_2\text{O}_3/\text{Ga}_2\text{O}_3$ interfaces synthesized by ALD. We would expect sputter deposition to create even more surface disorder. Interestingly, the measured offsets are also different than predicted by the difference in electron affinity between the Al_2O_3 and the Ga_2O_3 , which points to an important role for interfacial charge and trap states [23].

4. Summary and conclusions

The alignment at $\text{Al}_2\text{O}_3/\text{Ga}_2\text{O}_3$ heterojunctions is found to be dependent on how the dielectric was deposited. For ALD Al_2O_3 , it has a nested gap alignment of band offsets with a valence band offset of 0.07 eV and a conduction band offset of 2.23 eV determined from XPS measurements, while for sputtered Al_2O_3 on

Table 1

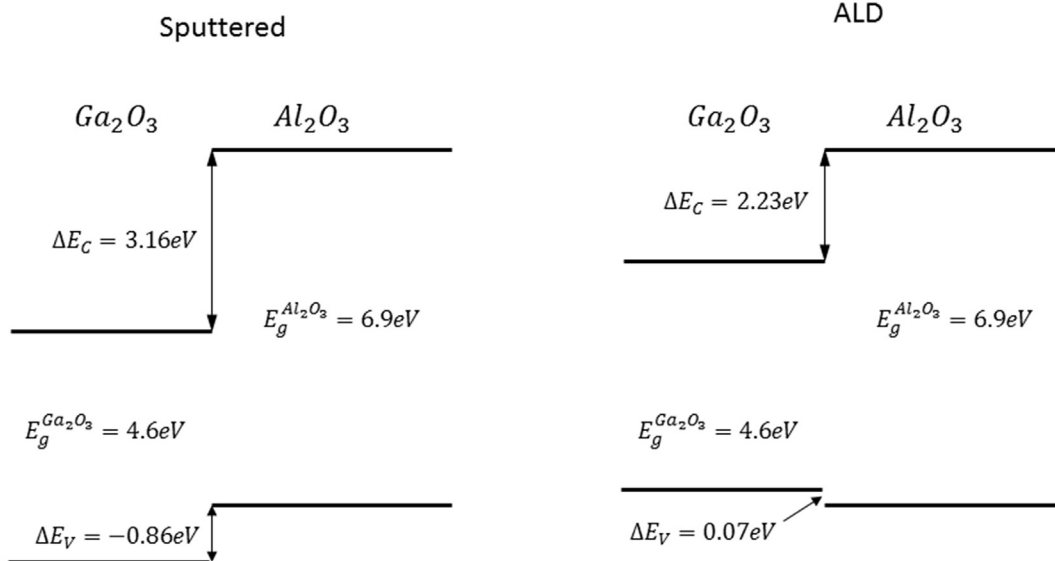
Values of band offsets determined in these experiments (eV).

Reference Ga ₂ O ₃					Reference Al ₂ O ₃			Thin Al ₂ O ₃ on Ga ₂ O ₃	
Ga ₂ O ₃ metal core	Ga ₂ O ₃ VBM	Metal Core level	Metal core - Ga ₂ O ₃ VBM	Deposition Method	Al ₂ O ₃ VBM	Al 2p core level	Al 2p - 2p VBM	Delta Core Levels Ga 2p _{3/2} - Al 2p	Valence band offset
Ga2p _{3/2}	3.20	1118.10	1114.90	ALD	3.25	74.40	71.15	1043.68	0.07
				Sputter	2.58	74.33	71.75	1044.01	-0.86

$$\Delta E_C = E_g^{Al_2O_3} - E_g^{Ga_2O_3} - \Delta E_V$$

$$\Delta E_C = 6.9\text{eV} - 4.6\text{eV} - (-0.86\text{eV}) = 3.16\text{eV} \quad \text{Sputtered}$$

$$\Delta E_C = 6.9\text{eV} - 4.6\text{eV} - 0.07\text{eV} = 2.23\text{eV} \quad \text{ALD}$$

**Fig. 6.** Band diagrams for Al₂O₃/Ga₂O₃ heterostructures in which the Al₂O₃ was deposited by sputtering or ALD.

the same Ga₂O₃, there is a type II alignment with a conduction band offset of -0.86 eV and a conduction band offset of 3.16 eV. The conduction band offsets in either case are large and provide excellent electron confinement, but the valence band offsets are smaller than desirable for limiting hole transport. The main result of this work is that the band alignment of a common dielectric on Ga₂O₃, measured under the same conditions, is quite different depending on the dielectric deposition method. This study is a cautionary tale of why the literature can show significant variations in reported band offsets for heterostructures.

Acknowledgments

The project or effort depicted was also sponsored by the Department of the Defense, Defense Threat Reduction Agency, HDTRA1-17-1-011, monitored by Jacob Calkins. The content of the information does not necessarily reflect the position or the policy of the federal government, and no official endorsement should be inferred. The research at Dankook was supported by the Basic Science Research Program through the National Research Foundation of Korea (NRF) funded by the Ministry of Education (2014R1A1A4A01008877, 2015R1D1A1A01058663), and Nano Material Technology Development Program through the National Research Foundation of Korea (NRF) funded by the Ministry of

Science, ICT and Future Planning (2015M3A7B7045185). Part of the work at Tamura was supported by “The research and development project for innovation technique of energy conservation” of the New Energy and Industrial Technology Development Organization, Japan. We also thank Dr. Kohei Sasaki from Tamura Corporation for fruitful discussions.

References

- [1] A. Kuramata, K. Koshi, S. Watanabe, Y. Yamaoka, T. Masui, S. Yamakoshi, High-quality β-Ga₂O₃ single crystals grown by edge-defined film-fed growth, Jpn. J. Appl. Phys. 55 (2016) 1202A2.
- [2] Zbigniew Galazka, Reinhard Uecker, Detlef Klimm, Klaus Irmscher, Martin Naumann, Mike Pietsch, Albert Kwasniewski, Rainer Bertram, Steffen Ganschow, Matthias Bickermann, Scaling-up of bulk β-Ga₂O₃ single crystals by the czochralski method, ECS J. Solid State Sci. Technol. 6 (2017) Q3007.
- [3] Michele Baldiniz, Martin Albrecht, Andreas Fiedler, Klaus Irmscher, Robert Schewski, Günter Wagner, Si- and Sn-Doped homoepitaxial β-Ga₂O₃ layers grown by MOVPE on (010)-oriented substrates, ECS J. Solid State Sci. Technol. 6 (2017) Q3040.
- [4] Masataka Higashiwaki, Kohei Sasaki, Hisashi Murakami, Yoshinao Kumagai, Akinoi Koukitu, Akito Kuramata, Takekazu Masui, Shigenobu Yamakoshi, Recent progress in Ga₂O₃ power devices, Semicond. Sci. Technol. 31 (2016) 034001.
- [5] A.M. Armstrong, M.H. Crawford, A. Jayawardena, A. Ahyi, S. Dhar, Role of self-trapped holes in the photoconductive gain of β-gallium oxide Schottky diodes, J. Appl. Phys. 119 (2016) 103102.
- [6] M. Higashiwaki, K. Sasaki, A. Kuramata, T. Masui, S. Yamakoshi, Development

- of gallium oxide power devices, *Phys. Stat. Solidi A* 211 (2014) 21.
- [7] Kelson D. Chabak, Neil Moser, Andrew J. Green, Dennis E. Walker Jr., Stephen E. Tetlak, Eric Heller, Antonio Crespo, Robert Fitch, Jonathan P. McCandless, Kevin Leedy, Michele Baldini, Gunter Wagner, Zbigniew Galazka, Xiuling Li, Gregg Jessen, Enhancement-mode β -Ga₂O₃ wrap-gate fin field-effect transistors on native (100) β -Ga₂O₃ substrate with high breakdown voltage, *Appl. Phys. Lett.* 109 (2016) 213501.
- [8] Andrew J. Green, Kelson D. Chabak, Eric R. Heller, Robert C. Fitch Jr., Michele Baldini, Andreas Fiedler, Klaus Irmischer, Gunter Wagner, Zbigniew Galazka, Stephen E. Tetlak, Antonio Crespo, Kevin Leedy, Gregg H. Jessen, 3.8-MV/cm breakdown strength of MOVPE-grown Sn-Doped β -Ga₂O₃ MOSFETs, *IEEE Electron Dev. Lett.* 37 (2016) 902.
- [9] M.H. Wong, K. Sasaki, A. Kuramata, S. Yamakoshi, M. Higashiwaki, Field-plated Ga₂O₃ MOSFETs with a breakdown voltage of over 750 V, *IEEE Electr. Dev. Lett.* 37 (2016) 212.
- [10] S. Oh, G. Yang, Jihyun Kim, Electrical characteristics of vertical Ni/ β -Ga₂O₃ schottky barrier diodes at high temperatures, *ECS J. Solid State Sci. Technol.* 6 (2017) Q3022.
- [11] M.J. Tadjer, N.A. Mahadik, V.D. Wheeler, E.R. Glaser, L. Ruppalt, A.D. Koehler, K.D. Hobart, C.R. Eddy Jr., F.J. Kub, A (001) β -Ga₂O₃ MOSFET with +2.9 V threshold voltage and HfO₂ gate dielectric, *ECS J. Solid State Sci. Technol.* 5 (2016) 468.
- [12] M. Higashiwaki, K. Sasaki, T. Kamimura, M.H. Wong, D. Krishnamurthy, A. Kuramata, T. Masui, S. Yamakoshi, Depletion-mode Ga₂O₃ metal-oxide-semiconductor field-effect transistors on β -Ga₂O₃ (010) substrates and temperature dependence of their device characteristics, *Appl. Phys. Lett.* 103 (2013) 123511.
- [13] M. Higashiwaki, K. Konishi, K. Sasaki, K. Goto, K. Nomura, Q.T. Thieu, R. Togashi, H. Murakami, Y. Kumagai, B. Monemar, A. Koukitu, A. Kuramata, S. Yamakoshi, Temperature-dependent capacitance–voltage and current–voltage characteristics of Pt/Ga₂O₃ (001) Schottky barrier diodes fabricated on n^- -Ga₂O₃ drift layers grown by halide vapor phase epitaxy, *Appl. Phys. Lett.* 108 (2016) 133503.
- [14] K. Konishi, K. Goto, H. Murakami, Y. Kumagai, A. Kuramata, S. Yamakoshi, M. Higashiwaki, 1-kV vertical Ga₂O₃ field-plated Schottky barrier diodes, *Appl. Phys. Lett.* 110 (2017) 103506.
- [15] W.S. Hwang, A. Verma, H. Peelaers, V. Protasenko, S. Ruvimov, H. (Grace) Xing, A. Seabaugh, W. Haensch, C. Van de Walle, Z. Galazka, M. Albrecht, R. Fornari, D. Jena, High-voltage field effect transistors with wide-bandgap β -Ga₂O₃ nanomembranes, *Appl. Phys. Lett.* 104 (2014) 203111.
- [16] Shihyun Ahn, Fan Ren, Janghyuk Kim, Sooyeon Oh, Jihyun Kim, Michael A. Mastro, S.J. Pearton, Effect of front and back gates on β -Ga₂O₃ nano-belt field-effect transistors, *Appl. Phys. Lett.* 109 (2016) 062102.
- [17] Janghyuk Kim, Sooyeon Oh, Michael Mastro, Jihyun Kim, Exfoliated β -Ga₂O₃ nano-belt field-effect transistors for air-stable high power and high temperature electronics, *Phys. Chem. Chem. Phys.* 18 (2016) 15760.
- [18] M. Mohamed, K. Irmischer, C. Janowitz, Z. Galazka, R. Manzke, R. Fornari, Schottky barrier height of Au on the transparent semiconducting oxide β -Ga₂O₃, *Appl. Phys. Lett.* 101 (2012) 132106.
- [19] Q. He, W. Mu, H. Dong, S. Long, Z. Jia, H. Lv, Q. Liu, M. Tang, X. Tao, M. Liu, Schottky barrier diode based on β -Ga₂O₃ (100) single crystal substrate and its temperature -dependent electrical characteristics, *Appl. Phys. Lett.* 110 (2017) 093503.
- [20] M.J. Tadjer, V.D. Wheeler, D.I. Shahin, C.R. Eddy, F.J. Kub, Thermionic emission analysis of TiN and Pt schottky contacts to β -Ga₂O₃, *ECS J. Solid State Sci. Technol.* 6 (2017) 165.
- [21] K. Konishi, T. Kamimura, M.H. Wong, K. Sasaki, A. Kuramata, S. Yamakoshi, M. Higashiwaki, Large conduction band offset at SiO₂/ β -Ga₂O₃ heterojunction determined by X-ray photoelectron spectroscopy, *Phys. Status Solidi B* 253 (2016) 623.
- [22] T. Kamimura, K. Sasaki, M.H. Wong, D. Krishnamurthy, A. Kuramata, T. Masui, S. Yamakoshi, M. Higashiwaki, Band alignment and electrical properties of Al₂O₃/ β -Ga₂O₃ heterojunctions, *Appl. Phys. Lett.* 104 (2014) 192104.
- [23] Ting-Hsiang Hung, Kohei Sasaki, Akito Kuramata, Digbijoy N. Nath, Pil Sung Park, Craig Polchinski, Siddharth Rajan, Energy band line-up of atomic layer deposited Al₂O₃ on β -Ga₂O₃, *Appl. Phys. Lett.* 104 (2014) 162106.
- [24] M. Hattori, T. Oshima, R. Wakabayashi, K. Yoshimatsu, K. Sasaki, T. Masui, A. Kuramata, S. Yamakoshi, K. Horiba, H. Kumigashira, A. Ohtomo, Epitaxial growth and electrical properties of γ -Al₂O₃ (110) films on β -Ga₂O₃ substrates, *Jpn. J. Appl. Phys.* 55 (2016) 1202B6.
- [25] Y. Jia, K. Zheng, J.S. Wallace, J.A. Gardella, U. Singisetti, Spectroscopic and electrical calculation of band alignment between atomic layer deposited SiO₂ and β -Ga₂O₃ (-201), *Appl. Phys. Lett.* 106 (2016) 102107.
- [26] Virginia D. Wheeler, David I. Shahin, Marko J. Tadjer, Charles R. Eddy Jr., Band alignments of atomic layer deposited ZrO₂ and HfO₂ high-k dielectrics with (-201) β -Ga₂O₃, *ECS J. Solid State Sci. Technol.* 6 (2017) Q3052.
- [27] David C. Hays, B.P. Gila, S.J. Pearton, Energy band offsets of dielectrics on InGaZnO₄, *Appl. Phys. Rev.* 4 (2017) 021301.
- [28] David C. Hays, B.P. Gila, S.J. Pearton, Andres Trucco, Ryan Thorpe, F. Ren, Effect of deposition conditions and composition on band offsets in atomic layer deposited Hf_xSi_{1-x} O_y on InGaZnO₄, *J. Vac. Sci. Technol. B35* (2017) 011206.
- [29] Hyun Cho, E.A. Douglas, A. Scheurmann, B.P. Gila, V. Craciun, E.S. Lambers, S.J. Pearton, F. Ren, Al₂O₃/InGaZnO₄ heterojunction band offsets by x-ray photoelectron spectroscopy, *Electrochim. Solid-State Lett.* 14 (2011) H431.
- [30] E.A. Kraut, R.W. Grant, J.R. Waldrop, S.P. Kowalczyk, Precise determination of the valence-band edge in x-ray photoemission spectra: application to measurement of semiconductor interface potentials, *Phys. Rev. Lett.* 44 (1980) 1620.
- [31] E. Bersch, M. Di, S. Consiglio, R.D. Clark, G.J. Leusinkand, A.C. Diebold, Complete band offset characterization of the HfO₂/SiO₂/Si stack using charge corrected x-ray photoelectron spectroscopy, *J. Appl. Phys.* 107 (2010) 043702.
- [32] H.C. Shin, D. Tahir, S. Seo, Y.R. Denny, S.K. Oh, H.J. Kang, S. Heo, J.G. Chung, J.C. Lee, S. Tougaard, Reflection electron energy loss spectroscopy for ultrathin gate oxide materials, *Surf. Interface Anal.* 44 (2012) 623.
- [33] Grzegorz Greczynski, Lars Hultman, C 1s peak of adventitious carbon aligns to the vacuum level: dire consequences for Material's bonding assignment by photoelectron spectroscopy, *Chem. Phys. Chem.* 18 (2017) 1.
- [34] P.H. Carey IV, F. Ren, David C. Hays, B.P. Gila, S.J. Pearton, Soohwan Jang, Akito Kuramata, Valence and conduction band offsets in AZO/Ga₂O₃ heterostructures, *Vacuum* 141 (2017) 103.
- [35] X. Guo, H. Zheng, S.W. King, V.V. Afanas'ev, M.R. Baklanov, J.-F.D. Marneffe, Y. Nishi, J.L. Shohet, Defect-induced bandgap narrowing in low-k dielectrics, *Appl. Phys. Lett.* 107 (2015) 082903.
- [36] A. Zur, T.C. McGill, Band offsets, defects, and dipole layers in semiconductor heterojunctions, *J. Vac. Sci. Technol. B* 2 (1984) 440.
- [37] H.-K. Dong, L.-B. Shi, Impact of native defects in the high dielectric constant oxide HfSiO₄ on MOS device performance, *Chin. Phys. Lett.* 33 (2016) 016101.
- [38] J. Xu, Y. Teng, F. Teng, Effect of surface defect states on valence band and charge separation and transfer efficiency, *Sci. Rep.* 6 (2016) 32457.
- [39] M. Yang, R.Q. Wu, Q. Chen, W.S. Deng, Y.P. Feng, J.W. Chai, J.S. Pan, S.J. Wang, Impact of oxide defects on band offset at GeO₂/Ge interface, *Appl. Phys. Lett.* 94 (2009) 142903.
- [40] S. Rahimnejad, J.H. He, W. Chen, K. Wu, G.Q. Xu, Tuning the electronic and structural properties of WO₃ nanocrystals by varying transition metal tungstate precursors, *RSC Adv.* 4 (2014) 62423.
- [41] A.K. Rumaiz, B. Ali, A. Ceylan, M. Boggs, T. Beebe, S.I. Shah, Experimental studies on vacancy induced ferromagnetism in undoped TiO₂, *Solid State Commun.* 144 (2007) 334.
- [42] A. Klein, Energy band alignment in chalcogenide thin film solar cells from photoelectron spectroscopy, *J. Phys. C. Solid* 27 (2015) 134201.
- [43] A. Klein, Energy band alignment at interfaces of semiconducting oxides: a review of experimental determination using photoelectron spectroscopy and comparison with theoretical predictions by the electron affinity rule, charge neutrality levels and the common anion rule, *Thin Solid Films* 520 (2012) 372.
- [44] J. Robertson, S.J. Clark, Limits to doping in oxides, *Phys. Rev. B* 83 (2011) 075205.
- [45] F. Chen, R. Schaffranek, S. Li, W. Wu, A.J. Klein, Energy band alignment between Pb(Zr,Ti)O₃ and high and low work function conducting oxides—from hole to electron injection, *J. Phys. D.* 43 (2010) 295301.
- [46] S. Li, F. Chen, R. Schaffranek, T.J.M. Bayer, K. Rachut, A. Fuchs, S. Siol, M. Weidner, M. Hohmann, V. Pfeifer, J. Morasch, C. Ghinea, E. Arveux, R. Gunzler, J. Gassmann, C. Korber, Y. Gassenbauer, F. Sauberlich, G.V. Rao, S. Payan, M. Maglione, C. Chirila, L. Pintilie, L. Jia, K. Ellmer, M. Naderer, K. Reichmann, U. Bottger, S. Schmelzer, R.C. Frunza, H. Ursic, B. Malic, W.-B. Wu, P. Erhart, A. Klein, Intrinsic energy band alignment of functional oxides, *Phys. Status Solidi Rapid Res. Lett.* 8 (2014) 571.